Cancer Therapy: Preclinical

Clinical Cancer Research

The Histone Deacetylase Inhibitor Abexinostat Induces Cancer Stem Cells Differentiation in Breast Cancer with Low *Xist* Expression

Marion A. Salvador[1,3,4], Julien Wicinski[1,3,4], Olivier Cabaud[1,3,4], Yves Toiron[3,4,5], Pascal Finetti[1,3,4], Emmanuelle Josselin[1,3,4], Hélène Lelièvre[6], Laurence Kraus-Berthier[6], Stéphane Depil[6], François Bertucci[1,3,4], Yves Collette[3,4,5], Daniel Birnbaum[1,3,4], Emmanuelle Charafe-Jauffret[1,2,3,4], and Christophe Ginestier[1,3,4]

Abstract

Purpose: Cancer stem cells (CSC) are the tumorigenic cell population that has been shown to sustain tumor growth and to resist conventional therapies. The purpose of this study was to evaluate the potential of histone deacetylase inhibitors (HDACi) as anti-CSC therapies.

Experimental Design: We evaluated the effect of the HDACi compound abexinostat on CSCs from 16 breast cancer cell lines (BCL) using ALDEFLUOR assay and tumorsphere formation. We performed gene expression profiling to identify biomarkers predicting drug response to abexinostat. Then, we used patient-derived xenograft (PDX) to confirm, *in vivo*, abexinostat treatment effect on breast CSCs according to the identified biomarkers.

Results: We identified two drug-response profiles to abexinostat in BCLs. Abexinostat induced CSC differentiation in low-dose sensitive BCLs, whereas it did not have any effect on the CSC population from high-dose sensitive BCLs. Using gene expression profiling, we identified the long noncoding RNA *Xist* (X-inactive specific transcript) as a biomarker predicting BCL response to HDACi. We validated that low *Xist* expression predicts drug response in PDXs associated with a significant reduction of the breast CSC population.

Conclusions: Our study opens promising perspectives for the use of HDACi as a differentiation therapy targeting the breast CSCs and identified a biomarker to select patients with breast cancer susceptible to responding to this treatment. *Clin Cancer Res; 19(23); 6520–31. ©2013 AACR.*

Introduction

Acetylation of histone proteins controls transcription and regulation of genes involved in cell-cycle control, proliferation, DNA repair and differentiation (1, 2). Unsurprisingly, the expression of histone deacetylases (HDAC) is frequently altered in several malignancies (3), including breast cancer, and pharmacologic inhibitors (histone deacetylase inhibitor; HDACi) have been proposed as an alternate therapy to conventional therapeutics in solid malignancies.

Resistance to conventional therapeutic agents in cancer may be sustained by a fraction of cancer cells within the tumor, the cancer stem cells (CSC), which are able to self-renew and differentiate, giving rise to the bulk of the tumor (4). In breast cancer, in particular, this population has been shown to resist to conventional chemotherapy and radiation, suggesting that it will be imperative to target all CSC subsets within the tumor to prevent relapse and metastasis (5). Different features of CSCs have been explored in recent targeting strategies including quiescence, self-renewal, or radioresistance pathways (6). It has been demonstrated that inhibition of key signaling pathways involved in breast CSCs self-renewal reduces breast tumorigenesis and metastasis (6). Among the different anti-CSC therapeutic strategies recently developed, differentiation therapy using "epidrugs" remains poorly explored in solid tumors. Differentiation therapy aims at favoring differentiation over self-renewal programs in CSCs, inducing a depletion of the CSC population (7). Whether HDACis could influence CSCs fate remains unknown. However, during normal differentiation, the chromatin structure of stem cells undergoes major epigenetic modifications (8) with histone acetylation, which has been proposed to play a fundamental role in the control of cell-fate choice (9). The balance

Authors' Affiliations: [1]Institut national de la santé et de la recherche medicale (INSERM), CRCM, U1068, Laboratoire d'Oncologie Moléculaire; [2]Département de Biopathologie, Institut Paoli-Calmettes; [3]Aix Marseille Université, F-13007; [4]CNRS, CRCM, 7258; [5]INSERM, CRCM, U1068, TrGET, Marseille; and [6]Institut de Recherches Internationales Servier, Paris, France

Note: Supplementary data for this article are available at Clinical Cancer Research Online (http://clincancerres.aacrjournals.org/).

Corresponding Author: Christophe Ginestier, CRCM, U1068 Inserm, Department of Molecular Oncology, 27 Bd Leï Roure, BP 30059, 13273 Marseille. Phone: 33-491-22-35-09; Fax: 33-491-22-35-44; E-mail: christophe.ginestier@inserm.fr

doi: 10.1158/1078-0432.CCR-13-0877

Translational Relevance

Although the overall mortality for breast cancer has recently been declining, the survival of patients with recurrent or metastatic disease has not changed significantly over the past decades. Targeting the tumorigenic cancer stem cell (CSC) population is a prerequisite to improve breast cancer treatment. Among the different anti-CSC therapeutic strategies recently developed, differentiation therapy using "epidrugs" remains poorly explored in solid tumors. In this study, we demonstrate that the histone deacetylase inhibitor (HDACi) abexinostat may be used to induce differentiation of breast CSCs. Moreover, we identify a biomarker (*Xist* expression) that predicts tumor response to abexinostat treatment. Thus, the use of epidrugs such as HDACi may be an effective therapeutic approach to treat breast tumor with low *Xist* expression.

between histone acetylation/deacetylation by histone acetyltransferases (HAT)/HDACs is one of the main features of the "epigenetic memory" of a cell. Consequently, epidrug therapies modifying the histone code have been proposed for cancer treatment and more recently as potential anti-CSC therapies.

Forty years ago, the anticancer properties of HDACis were suggested through their capability to induce the differentiation of erythroleukemia cells (10). To date, HDACis have been used as differentiation therapy in several hematologic malignancies (11). More recently, HDACis were also reported to induce differentiation in endometrial stromal sarcoma cells (12), in liver cancer cell lines (13), and in small cell lung cancer cells (14). Differentiation in breast cancer has been described in response to HDACi in different cell line models. Suberoylanilide hydroxamic acid (SAHA) treatment induced a complete differentiation of MCF-7 cells with the induction of milk fat globule protein (15). Several HDACis are being tested in clinical studies as single agents in several solid tumor malignancies (16).

These compounds are only efficient at high concentrations. Thus, the effect of HDACis might, at least in part, be the results of nonspecific side effects rather than the consequences of inhibiting HDAC *per se*. Furthermore, there is no existing biomarker able to predict HDACi efficiency. Both improving our knowledge of HDACi biology and testing more efficient HDACi compounds could greatly impact the therapy success.

We studied the effect of HDAC inhibition on the breast CSC population, using the broad spectrum HDACi abexinostat, which has been developed to have a full pharmacologic effect at a nanomolar range (17). We identified, *in vitro* and *in vivo*, two types of response to abexinostat with either an induction of CSC differentiation in low-dose sensitive breast cancer cell lines (BCL) or no effect on the CSC population from high-dose sensitive BCLs. Moreover, we identified the long noncoding RNA (lncRNA) *Xist* (X-inactive specific transcript) as a potential biomarker predicting BCL response to HDACi. These results open promising perspectives for the use of HDACi as differentiation therapy targeting the CSC population of breast cancer with low *Xist* expression.

Results

Treatment with histone deacetylase inhibitor defines two drug-response profiles in breast cancer cell lines

A series of 16 BCLs representing the molecular diversity of breast cancers were exposed for 72 hours to increasing concentrations (150 nmol/L–2.5 μM) of the HDACi abexinostat (Supplementary Table S1). According to the Gaussian Mixture Model (GMM) analysis, nine BCLs were classified as sensitive to low dose of abexinostat with an IC_{50} comprised between 170 and 460 nmol/L, whereas seven were classified as sensitive to high dose with an IC_{50} superior to 700 nmol/L (IC_{50} range: 715–1,650 nmol/L; Fig. 1 and Supplementary Fig. S1). These two drug-response profiles were similar when using other HDACi compounds (SAHA and valproic acid; Supplementary Fig. S2). To explain this differential response to HDACi treatment, we grouped the BCLs according to their molecular features. None of the molecular parameters tested could predict response to HDACi (Supplementary Fig. S3). To exclude an indirect cytotoxic effect of HDACi treatment, we compared our abexinostat response profile with the one of docetaxel, a conventional chemotherapeutic agent used to treat breast cancer. Abexinostat and docetaxel drug-response profiles were totally distinct, suggesting that HDACi treatment had a specific effect (Supplementary Fig. S3B). We measured histone deacetylase activity in our BCL series before and after the abexinostat treatment (Supplementary Fig. S4A and S4B). Intrinsic histone deacetylase activity was not correlated to BCL's drug-response profile,

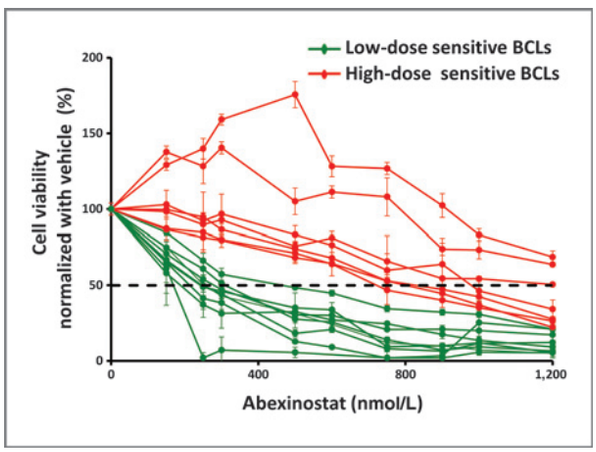

Figure 1. BCLs display two drug-response profiles to abexinostat. Cell viability was measured with an MTS assay after 72 hours of treatment for 16 BCLs ($n = 12$). Dotted line allows determination of IC_{50} for each BCL. BCLs sensitive to low doses of abexinostat are represented with green curves; BCLs sensitive to high doses of abexinostat are represented with red curves. Error bars represent mean ± SD.

and both low-dose sensitive and high-dose sensitive BCLs presented a similar extinction of HDAC activity after treatment ($P < 0.01$; t test). Moreover, abexinostat treatment induced a significant increase of acetylated proteins (histone H3 and α-tubulin) after 24 hours of drug exposure (Supplementary Fig. S4C and S4D). Altogether, these results indicate that abexinostat treatment inhibits specifically HDAC activity in all BCLs tested, independently of their drug-response profile.

Treated cells exhibit differential cell-cycle progression according to their drug-response profiles

To determine whether drug-response profiles were dependent on apoptosis induction, we measured caspase-3/7 activation after abexinostat treatment. Surprisingly, low-dose sensitive BCLs did not present apoptosis induction, whereas high-dose sensitive BCLs did present an activation of caspase-3/7 after 48 hours of abexinostat treatment ($P < 0.01$; t test; Fig. 2A). Because the abexinostat inhibitory effect observed in low-dose sensitive BCLs could not be explained by a massive cell death, we measured cell growth kinetic. As expected, the proliferation rate of high-dose sensitive BCLs decreased after 48 hours of drug exposition. Low-dose sensitive BCLs showed a transient stop in cell growth kinetic after 24 hours of treatment followed by a recovery of cell proliferation (Fig. 2B). These results suggest that abexinostat effect on low-dose sensitive BCLs may be due to a perturbation of cell-cycle progression, whereas it induced apoptosis in high-dose sensitive BCLs. To test this hypothesis, we analyzed the cell-cycle status of four BCLs (two low-dose sensitive: SK-BR-7, MDA-MB-231; two high-dose sensitive: MDA-MB-436, HCC1954) for different time points after abexinostat treatment at IC_{50}. Low-dose sensitive BCLs were transiently blocked in G_1–S phase after 24 hours ($P < 0.01$; t test), whereas high-dose sensitive BCLs presented a G_2–M cell-cycle arrest ($P < 0.01$; t test; Fig. 2C and D and Supplementary Fig. S5A and S5B). To confirm this result, we measured P21 and P27 protein expression

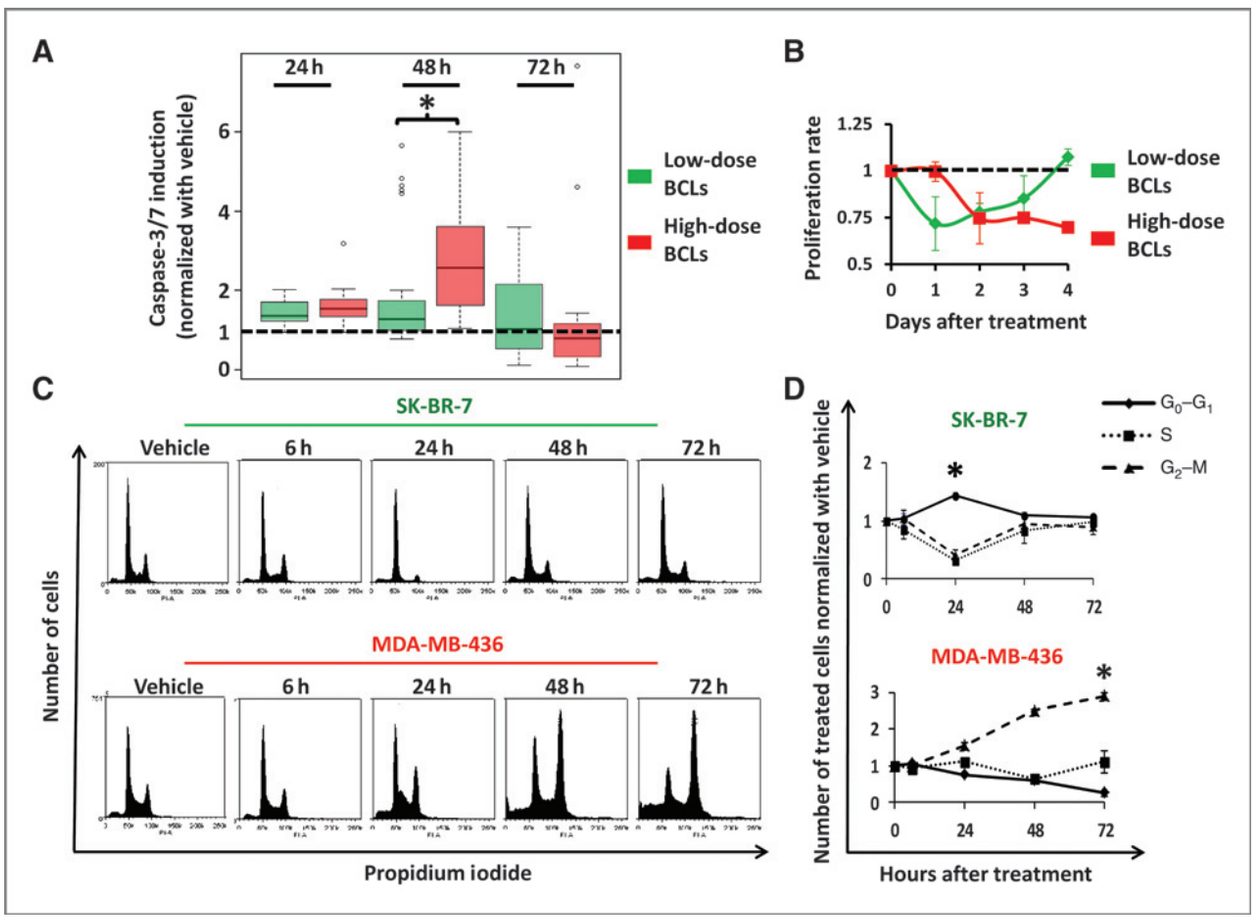

Figure 2. Cell-cycle progression was differentially altered by abexinostat according to drug-response profile. A, measurement of apoptosis induction by measuring caspase-3/7 activation in BCL panel (excluding MCF7) treated by abexinostat ($n = 3$; *, $P < 0.01$). B, cell proliferation was estimated using MTS viability test, and proliferation rate was calculated in 16 BCLs treated by abexinostat (high-dose sensitive BCLs: red curve; low-dose sensitive BCLs: green curve; $n = 3$). C, flow charts representing cell-cycle distribution of a low-dose sensitive BCL (SK-BR-7) and high-dose sensitive BCL (MDA-MB-436) along 72 hours of treatment. Quantifications of cells in each cell-cycle phase are represented in D ($n = 3$; *, $P < 0.01$). Similar results are reported for MDA-MB-231 and HCC1954 BCLs (Supplementary Fig. S6). Error bars represent mean ± SD.

using Western blot analysis (Supplementary Fig. S5C). Both proteins are checkpoint regulators of cell-cycle progression whose expression prevents G_1 to S phase transition. Western blot analysis showed that abexinostat induced P21 and P27 expression only in low-dose sensitive BCLs and in a transient fashion.

Histone deacetylase inhibitors modulate breast cancer stem cells

To explore whether drug-response profiles were related to an effect on the breast CSC population, we evaluated the CSC population on BCLs treated with HDACis with two different techniques, the ALDEFLUOR assay and the tumorsphere formation assay. We have previously demonstrated that BCLs contain populations with stem cell properties that can be isolated upon their aldehyde dehydrogenase activity as assessed by the ALDEFLUOR assay (18). Moreover, the capacity to generate a colony in nonadherent culture conditions (tumorsphere) has been shown to be an intrinsic property of CSCs (19). Seven BCLs (three low-dose sensitive: SUM149, SUM159, SK-BR-7; four high-dose sensitive: BrCa-MZ-01, S68, MDA-MB-436, HCC1954) were treated for 72 hours with abexinostat (IC_{50}). For each low-dose sensitive BCL tested, we observed a decrease of the CSC population with twice less ALDEFLUOR-positive cells and tumorspheres formed after treatment ($P < 0.05$; *t* test; Fig. 3). Conversely, high-dose sensitive BCLs treated with abexinostat presented a moderate increase of the ALDEFLUOR-positive population and no effect on tumorsphere formation. Similar results were observed using other HDACi compounds (Supplementary Fig. S6; $P < 0.05$; *t* test).

We next evaluated the effect of two abexinostat structurally related compounds (S78730, carboxylic acid derivative; S78731, amide derivative) lacking HDAC inhibitory properties. This kind of approach has already been used with other HDACis to demonstrate the specificity of the anti-HDAC activity effect (20–22). Interestingly, both derivatives did not have any effect on cell growth or on CSC population (Supplementary Fig. S7). Altogether these results suggest that the proportion of breast CSCs is modulated by histone acetylation.

Abexinostat treatment induces CSC differentiation in low-dose sensitive BCLs

HDACi treatment may affect the breast CSC population through the induction of maturation process (10, 15). Therefore, we studied the protein expression of different differentiation markers by immunofluorescence, including CK5/6 and CK14 (basal markers), vimentin and E-cadherin (mesenchymal markers), and CK8/18 (luminal marker). Observed by optical microscopy, low-dose sensitive BCLs treated with abexinostat exhibited important morphologic changes with cells increased in size and with a decreased nuclear/cytoplasmic ratio. Also, treated cells flattened and generated intercellular digitations and bridges. Figure 4A shows newly formed cell clusters after abexinostat treatment. These morphologic changes were accompanied by a modification of phenotypic profiles. All BCLs analyzed presented a strong overexpression of the luminal marker

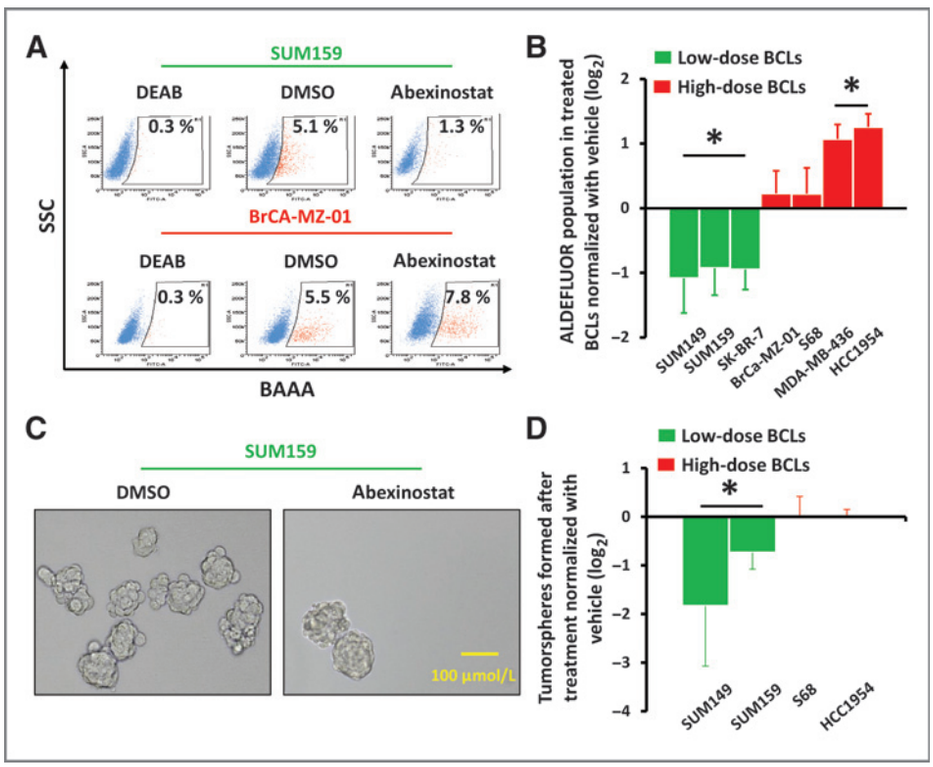

Figure 3. The CSC population is differentially modulated according to abexinostat-response profile. A–D, the effect of abexinostat on the CSC population was assessed using ALDEFLUOR assay (A and B) and tumorsphere formation (C and D). Representative flow charts for ALDEFLUOR assay (A) and pictures of tumorspheres (C) are presented. ($n = 6$; *, $P < 0.05$.) Error bars represent mean ± SD.

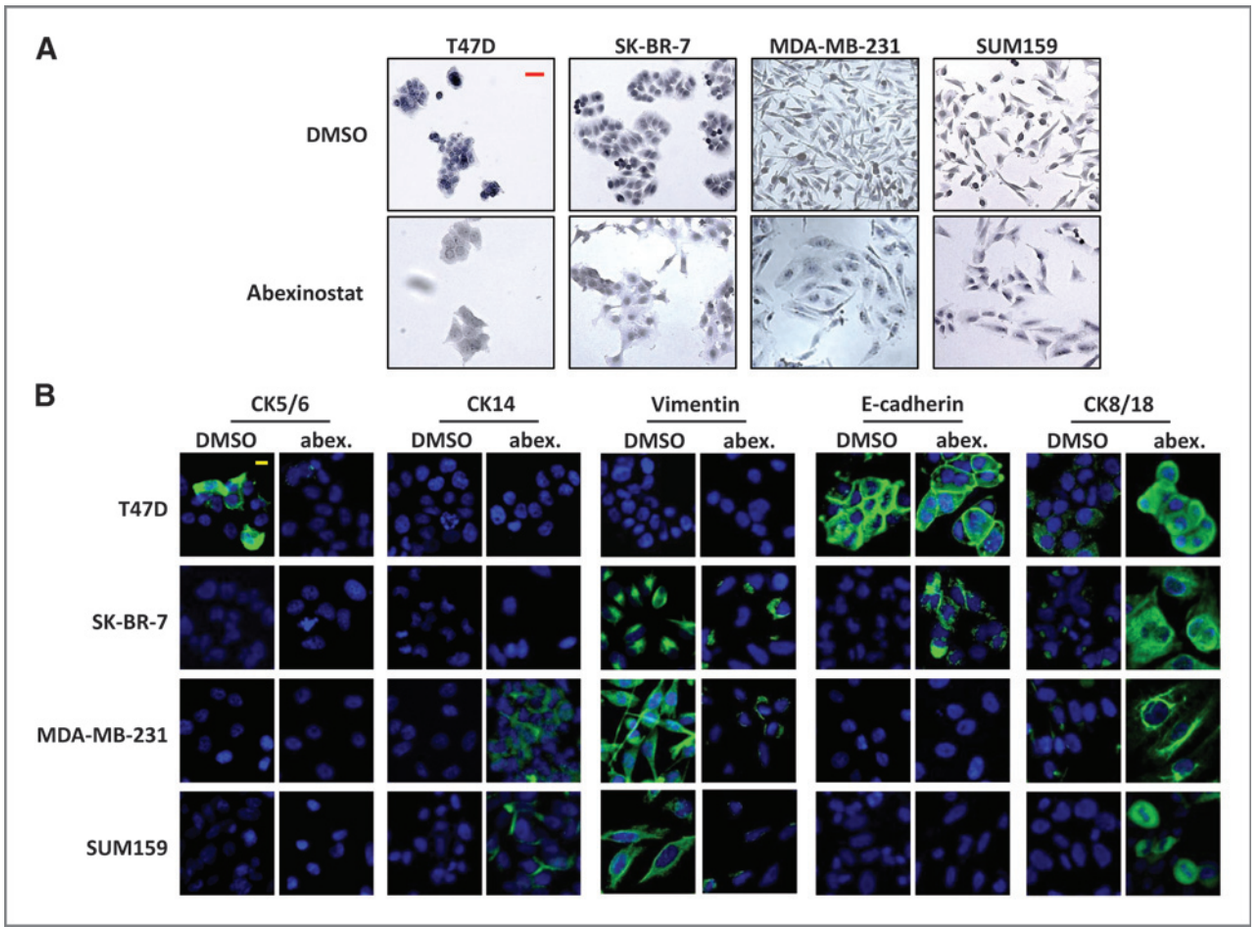

Figure 4. Abexinostat induces CSC differentiation in low-dose sensitive BCLs. A, optical microscopy showed that morphology of cells of four representative low-dose sensitive BCLs changed after 72 hours of treatment and cells formed large cell clusters. B, cell differentiation was monitored by measuring expression of differentiation markers using immunofluorescent staining (green staining); nuclei were counterstained using 4′,6-diamidino-2-phenylindole (DAPI; blue staining). Abexinostat treatment induces a modification of phenotypic profile. Scale bar = 10 μm.

CK8/18 after HDACi treatment (Fig. 4B and Supplementary Table S2). The mesenchymal marker vimentin was lost in BCLs from the mesenchymal molecular subtype, and E-cadherin expression was induced in SK-BR-7 BCL, suggesting a reverse epithelial-to-mesenchymal transition. In the luminal BCL T47D, the small CK5/6-positive cell population, previously identified as containing the tumor-initiating cell population (23), was totally eradicated in treated cells. We also noted an induction of CK14 expression in MDA-MB-231 and SUM159 mesenchymal BCLs. In summary, our data suggest that HDACi treatment induces differentiation in low-dose sensitive BCLs, consistent with the decrease of the CSC population observed in these cell lines.

Expression of *Xist* lncRNA predicts drug response to abexinostat

Targeting breast CSCs is presented as a promising strategy to improve breast cancer treatment. Our findings suggest that abexinostat could be used as a novel therapeutic strategy for breast cancer through the induction of CSC differentiation. However, a biomarker is needed to predict drug response of patients with breast cancer. None of the classical molecular parameters tested could predict BCL drug response (Supplementary Fig. S2). We established and compared the gene expression profiles of low-dose and high-dose sensitive BCLs. We identified the overexpression of *Xist* lncRNA up to 139-fold ($P < 0.00001$, t test; FDR q-val: 0.03) in high-dose sensitive BCLs compared with low-dose sensitive BCLs (Fig. 5A). We validated the cDNA microarrays results by quantifying *Xist* expression for each BCL using quantitative real-time PCR (qRT-PCR). *Xist* expression level was significantly correlated between both techniques [$r = 0.84$ (0.58–0.95), $P = 8.7E\text{-}05$; Fig. 5B]. We next confirmed that high-dose BCLs tended to be enriched in $Xist^{high}$ BCLs compared with low-dose sensitive BCLs ($P = 0.055$, Kruskal–Wallis rank-sum test; Fig. 5C). During the early steps of embryonic development, *Xist* randomly coats one X chromosome of females, allows the recruitment of chromatin modifiers, and reduces to silence an X chromosome over cell divisions. Consequently, the newly differentiated cell has one active (Xa) and one inactive (Xi) X

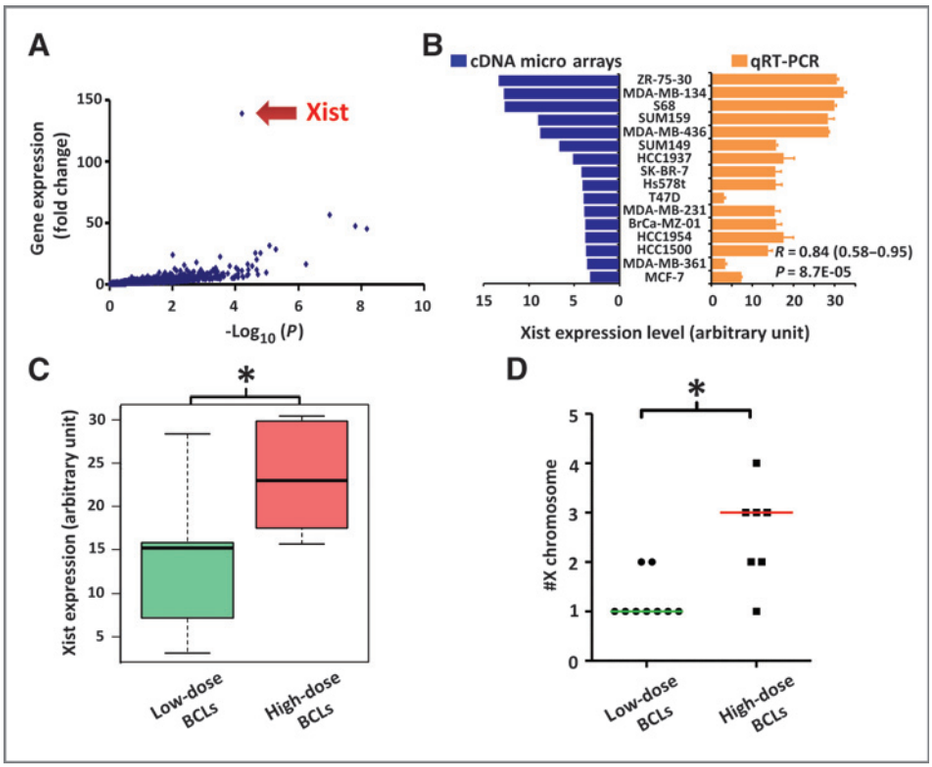

Figure 5. lncRNA *Xist* predicts response to abexinostat. A, transcriptomic analysis of low-dose sensitive BCLs versus high-dose sensitive BCLs. Results are plotted according to their gene differential expression between both BCL groups (*y* axis) and their corresponding statistical significance (*x* axis). *Xist* lncRNA (red arrow) was the most differentially expressed gene between the two BCL populations with an overexpression up to 139-fold ($P < 0.00001$; FDR *q*-val: 0.03) in high-dose sensitive BCLs. B, BCLs are classified according to increasing *Xist* expression level measured by cDNA microarrays; opposite the cDNA microarray measurements is a histogram presenting *Xist* expression level measured by qRT-PCR, $R = 0.84$ [(0.58–0.95), $P = 8.7E\text{-}5$; $n = 3$]. C, box plots represent *Xist* expression level in low-dose and high-dose sensitive BCLs measured by qRT-PCR. High-dose sensitive BCLs are significantly enriched in $Xist^{high}$ BCLs compared with low-dose sensitive BCLs ($n = 3$; *, $P = 0.055$). D, repartition of X chromosomes per cell in both BCL groups (*, $P = 0.0023$). Error bars represent mean ± SD.

chromosome (24). Several studies have reported genomic instability of X chromosomes (loss of Xi, duplications of Xa) and dysregulation of *Xist* in breast, ovarian, cervical, prostate cancers, testicular germ cell tumors, and lymphoma (25, 26). To evaluate whether a variation in X chromosomes number was related to *Xist* expression and drug response to abexinostat, we collected karyotype information for each BCL analyzed (Supplementary Table S3). We observed a strong correlation between X chromosomes number and drug response to abexinostat. Low-dose sensitive BCLs presented essentially X chromosome monosomy, whereas high-dose sensitive BCLs presented X chromosome normo- or polysomy ($P < 0.01$; *t* test; Fig. 5D). Altogether these results suggest that *Xist* lncRNA expression may be used as a biomarker to predict HDACi treatment effect on the breast CSC population.

Abexinostat treatment reduces the CSC population in patient-derived xenografts with low *Xist* expression

To confirm the impact of abexinostat treatment on the CSC population from breast cancers with low *Xist* expression, we utilized four different patient-derived xenografts (PDX) with distinct *Xist* expression level (CRCM226X, CRCM311X, $Xist^{low}$; CRCM392X, $Xist^{med}$; CRCM389X, $Xist^{high}$; Supplementary Fig. S8). Cells from these PDXs were transplanted orthotopically into fat pads of nonobese diabetic/severe combined immunodeficient (NOD/SCID) mice. Using these models, we previously demonstrated that the CSCs were contained in the ALDEFLUOR-positive population (27). We injected single cancer cells into fat pads of NOD/SCID mice and monitored tumor growth. When the tumor size was approximately 150 mm^3, we started treatment with abexinostat or docetaxel. Tumor growth was compared with that of placebo-treated controls. Docetaxel and abexinostat treatment had no or limited effect on PDXs growth (Fig. 6A). After 3 weeks of treatment, the animals were sacrificed and the proportion of ALDEFLUOR-positive CSCs was measured in each residual tumor (Fig. 6B). All PDX models presented an increase in the ALDEFLUOR-positive population isolated from docetaxel-treated tumors compared with the untreated control, in agreement with previous reports that described enrichment in the CSC population in residual tumors treated with conventional chemotherapy (28). In contrast, only PDXs with a low or medium *Xist* expression treated with abexinostat presented a two-fold decrease of the ALDEFLUOR-positive population

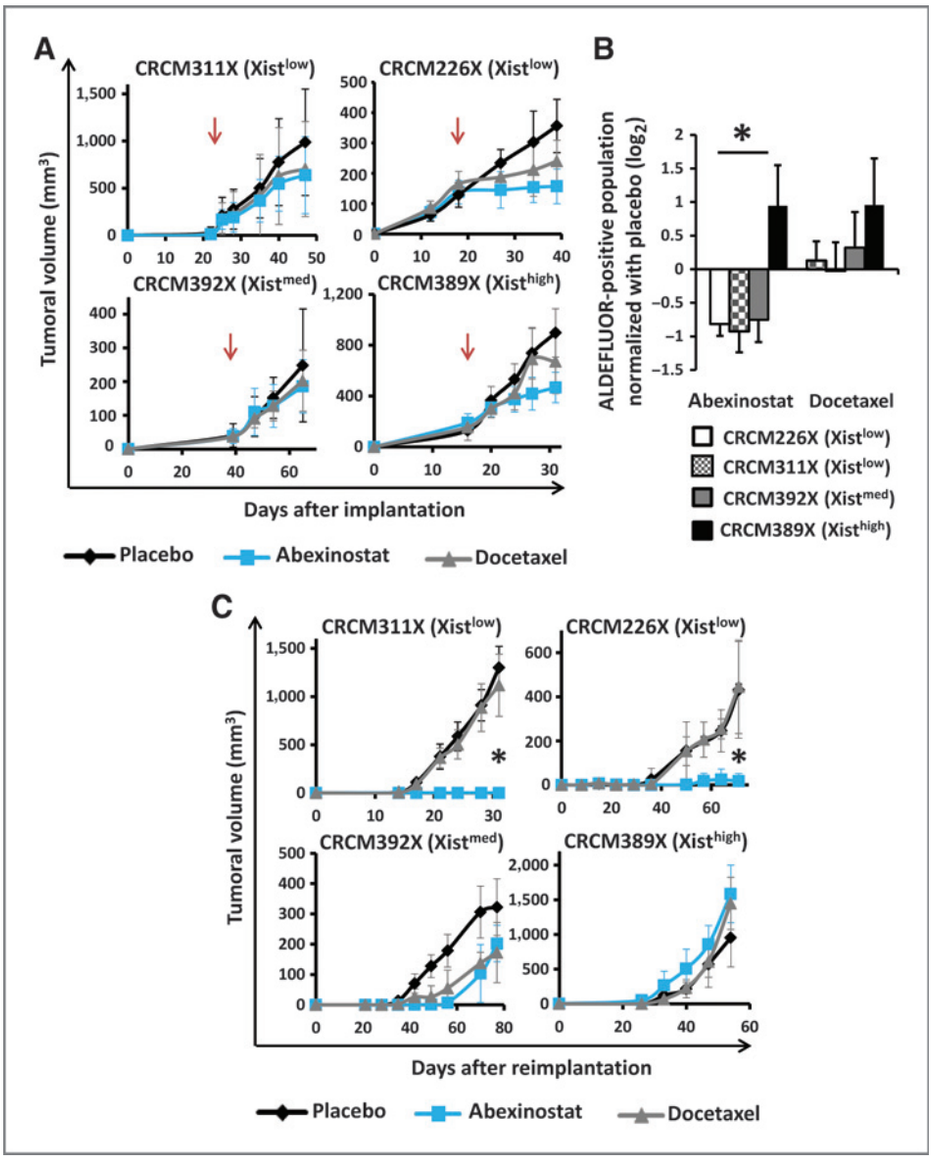

Figure 6. Abexinostat targets the CSC population in PDX with low *Xist* expression. A, tumor growth kinetic of PDX treated with docetaxel, abexinostat, or placebo (arrow indicates beginning of treatment) is presented for CRCM311X (*Xist*^{low}), CRCM226X (*Xist*^{low}), CRCM392X (*Xist*^{med}), and CRCM389X (*Xist*^{high}; $n = 4$). B, evaluation of the ALDEFLUOR-positive population in all four PDXs after 3 weeks of treatment with abexinostat or docetaxel. Results are represented normalized with the proportion of ALDEFLUOR-positive cells in the placebo-treated tumors ($n = 4$; *, $P < 0.05$). C, three-week treated PDXs were reimplanted into new mice and tumor growth was monitored. Tumor cells isolated from abexinostat-treated tumors were unable to regenerate a tumor for CRCM311X ($n = 8$; *, $P = 0.02$) and CRCM226X ($n = 4$; *, $P = 0.02$) PDX compared with the cells isolated from placebo- or docetaxel-treated PDXs. Error bars represent mean ± SD.

($P < 0.05$), whereas abexinostat treatment induced an increase of the ALDEFLUOR-positive population of CRCM389X (*Xist*^{high}). To functionally prove the reduction of the CSC population in the abexinostat-treated tumors with low *Xist* expression, we determined the ability of treated cells to form tumors *in vivo* by reimplantating cells from treated PDXs into secondary mice. Tumorigenicity is directly related to the presence of CSCs and this assay gives an estimate of the proportion of residual tumorigenic CSCs. For each treatment condition (placebo, abexinostat, docetaxel), 1,000 cells isolated from treated tumors were reimplanted. Cells isolated from abexinostat-treated PDXs showed an incapacity to regenerate a tumor for CRCM311X and CRCM226X (*Xist*^{low}), and a delay in tumor regrowth for CRCM392X (*Xist*^{med}) compared with the cells isolated from placebo-treated tumors ($P = 0.02$; Fig. 6C). In sharp contrast, cells isolated from docetaxel-treated tumors showed a tumor regrowth comparable with placebo-treated tumors. Interestingly, for CRCM389X (*Xist*^{high}), cells isolated from abexinostat-treated tumors presented a higher regrowth kinetic compared with cells isolated from docetaxel- and placebo-treated tumors (Fig. 6C). These results suggest that abexinostat treatment targets the CSC population *in vivo* and this effect is inversely correlated to *Xist* expression.

Discussion

Targeting CSCs within a tumor might be critical to prevent relapse and metastasis (5). CSC biology, such as expression of self-renewal and differentiation programs, is governed by epigenetic regulation (9). Thus, epigenetic

modulation using chromatin modifiers appears as an encouraging means to control CSC fate. The rationale for differentiation therapy is to disturb the balance between self-renewal and differentiation programs. Both inhibiting self-renewal and promoting differentiation would deplete the CSC pool and allow more differentiated tumor cells to be targeted by conventional treatments.

We observed two different response profiles to HDACi in BCLs. These profiles were associated with opposite effects on the breast CSC population. On one hand, the CSC population was decreased in low-dose sensitive BCLs in association with a cellular differentiation, suggesting that CSC decrease was mediated through the induction of a mesenchymal-to-epithelial transition. In addition, cell-cycle progression was transiently stopped with an accumulation in G_1 cell-cycle phase. This checkpoint before entering S phase, also called R point, has been defined as an important cell-cycle stage controlling stem cell fate allowing equilibrium between self-renewal and committed cell fate decision (29, 30). On the other hand, high-dose sensitive BCLs presented apoptosis induction with an accumulation of cells in G_2–M cell-cycle phase explaining cytotoxicity. As observed, when cancer cells are treated with cytotoxic agents, the CSC population in high-dose sensitive BCLs was not depleted after HDACi treatment. Altogether, these results suggested that modulation of histone acetylation of breast CSCs is able to alter their proportion. Interestingly, it has been shown that HDACis may promote either self-renewal or differentiation of embryonic stem cells depending on the "stem cell status" and dose used (31). Moreover, this opposite effect of HDACi treatment was previously observed in different malignant diseases where HDACi was described either as a differentiating agent (11–15, 32–34) or as an oncogenic factor promoting tumor growth and metastasis formation (35–37). Recently, a study screened 30 human epithelial cancer cell lines (comprising breast, liver, gastric, and lung cancer) for their HDACi sensitivity and reported two drug-response profiles with dramatic opposite effects: 13 out of the 30 cell lines presented increased cell migration and metastasis formation, whereas cell migration was inhibited in a dose-dependent manner in the other 17 cell lines (37). This dose-dependent dual effect of HDACi may be extended to other epidrugs and particularly to demethylating agents. Indeed, a low dose of decitabine on epithelial (breast and colon) and leukemic cancer cells had no immediate toxicity, induced memory response with cell differentiation and CSC depletion in serially transplanted mice, but a high dose triggered rapid DNA damages and cytotoxicity (38). If the molecular reason explaining the dual effect of epidrug treatment is unclear, we can postulate that the abexinostat effect is mediated at the cellular level through the modulation of the CSC pool.

A direct consequence of these observations is the need for reliable biomarkers predicting response to HDACi treatment to identify patients likely to benefit from these drugs. Because none of the conventional parameters tested were able to predict HDACi response in BCLs, we performed a gene expression analysis between our two BCL groups. This analysis revealed a differential expression of the lncRNA *Xist* with an overexpression of *Xist* in high-dose sensitive BCLs. *Xist* is responsible for X dosage compensation of X genes between males and females (24). Normally, X inactivation is initiated in early embryogenesis but recent reports identified instances where *Xist* is expressed and can initiate gene repression. A wider link between X chromosome inactivation and oncogenesis has been made in a number of studies observing a gain or loss of X chromosomes in tumor cells (25, 26). In our series of BCLs, *Xist* expression was correlated with X chromosome number ($P < 0.01$). We observed low *Xist* expression in BCLs with X mono- or disomy, whereas *Xist* overexpression was associated with X polysomy. Our results suggest that *Xist* expression may be used as a predictive biomarker for effectiveness of HDACi treatment through CSC differentiation. We confirmed, *in vivo*, this hypothesis by using PDX with distinct *Xist* expression. Only the PDX with low *Xist* expression displayed a significant decrease of its CSC population after abexinostat treatment, whereas HDACi treatment induced an increase of the CSC population in PDX with high *Xist* expression.

Why tumors with a low expression of *Xist* are hypersensitive to HDACis is not clear and need further investigation? Interestingly, *Xist* has recently been described as a predictive biomarker of response to cisplatin treatment in BRCA1-defective breast cancers (39). The authors proposed that low *Xist* expression may be a flag for genomic instability. Indeed, loss of Xi is the main cause explaining low *Xist* transcript level. Moreover, BRCA1-defective cells present chromosome segregation errors due to compromised spindle checkpoint (40). Consequently, BRCA1-deficient cancer cells are sensitive to treatment inducing DNA damage, and *Xist* expression would be a surrogate marker of DNA repair defect. Interestingly, it has been shown that HDAC enzymes are critically important to enable functional homologous recombination (HR) by controlling the expression of the *RAD51* gene and promoting the proper assembly of HR-directed subnuclear foci (41). Thus, HDACi may favor DNA damage in cancer cells with an important genomic instability such as cells presenting a low *Xist* gene expression. If this hypothesis can explain the low-dose sensitivity of BCLs with low *Xist* expression, it cannot explain the effect of HDACi treatment on the breast CSC population of these cell lines. One molecular mechanism debated for the role of *Xist* in tumorigenesis is its interaction with BRCA1 protein (42–46). Because BRCA1 has showed important role in the regulation of breast stem cell biology (47, 48), we can hypothesize that BRCA1 pathway is differentially regulated under HDACi treatment between low-dose and high-dose sensitive BCLs. Further studies are needed to decipher the precise underlying mechanism.

In conclusion, our study identifies for the first time a biomarker predicting breast cancer response to HDACi. It points out a lasting benefit of *Xist* low-expressing breast tumors treated with low-dose HDACi and the importance of epigenetic partners such as lncRNAs. LncRNAs said to be "dark matter" are more and more characterized (49) and increasing evidence imply them as critical in controlling

stem cell fate (50) and oncogenesis (51). Recently it was demonstrated, using *Xist*-deficient mice, that *Xist* loss results in X reactivation and consequent genome-wide changes that lead to hematologic cancer through hematopoietic stem cell aberrant maturation (52).

Ultimately, deciphering the role of lncRNAs in cancer biology will help improve cancer understanding and treatment.

Materials and Methods

Ethics statement

Use of anonymous human tissue samples was exempted from Institutional Review Board. Animal studies were approved by the INSERM office (Marseille, France) for Laboratory Animal Medicine.

Cell lines

A total of 16 BCLs were used for the study. The characteristic of the BCLs were previously described (refs. 53–55; Supporting Information).

Drugs

BCLs were continuously treated for 72 hours in adherent conditions with HDACi: abexinostat (also known as S78454, CRA-024781, or PCI-17481; Servier), SAHA (Cayman) and Valproic Acid (Sigma). For the experiments, abexinostat was prepared in a 23.1-mmol/L stock solution, SAHA in a 0.5-mol/L stock solution, in dimethyl sulfoxide (DMSO; Sigma) and stored at −20°C. Valproic acid was prepared in a 1 mol/L stock solution in PBS (Gibco) and stored at 4°C. For experiments, cells were treated with respective IC_{50}. BCLs were also continuously treated for 72 hours in adherent conditions with 5 μmol/L abexinostat derivatives, S78730 (carboxylic acid) and S78731 (amide). S78730 and S78731 were prepared in a 23.1 mmol/L stock solution in DMSO and stored at −20°C. DMSO or PBS were used as vehicle control (C < 0.1%).

Cell viability and proliferation

IC_{50} were evaluated using MTS assay (Promega) as described in the Supporting Information.

Histone deacetylase activity

The effect of abexinostat and abexinostat derivatives treatment on HDAC was assessed by measuring residual enzyme activity using HDAC-glow I/II assay (Promega). BCLs were plated in adherent conditions in 96-well plates at 10,000 cells per well. After 24 hours, cells were treated with abexinostat (respective IC_{50}) or abexinostat derivatives (5 μmol/L) or vehicle, and 1 hour later, HDACs inhibition was measured according to manufacturer's guidelines.

Immunoblotting

Cells were harvested in medium, washed in PBS, lysed in extraction buffer [1% v/v Triton X-100, 50 mmol/L Hepes, pH7.1 mmol/L EDTA, 1 mmol/L EGTA, 150 mmol/L NaCl, 100 mmol/L NaF, 1 mmol/L Na_3VO_4, one tablet of Complete inhibitor mix (Roche) per 25 mL buffer], and loaded onto SDS-PAGE. Blots were incubated with respective primary antibodies diluted in TBS and Tween20 (TBSt; containing 0.1% Tween20 and 5% nonfat milk) and incubated overnight at 4°C. Then blots were washed, incubated with appropriate secondary antibodies (1/10.000; Dako), and detected using SuperSignal West Pico Chemiluminescent Substrate (Pierce). Antibodies used were anti-acetylated histone 3 (1/1.000; AbCam), anti-acetylated α-tubulin (1/1.000; Sigma), anti-P21 (1/500; AbCam), anti-P27 (1/500; AbCam), anti- α-tubulin (1/2.000; Sigma).

Caspase activity assay

The effect of abexinostat treatment on apoptotic pathways was assessed by detecting caspase-3/7 activity using Caspase Glo 3/7 assay (Promega). The BCLs panel (excluding MCF7 that lacks functional caspase-3) was plated in adherent conditions in 96-well plates at 10,000 cells per well. After 24 hours, cells were treated with respective IC_{50} or vehicle. Caspase activity induction was measured 24, 48, and 72 hours later according to manufacturer's guidelines.

Cell-cycle analysis

Briefly, supernatant and adherent cells were harvested, washed, and suspended in 0.5 mL medium containing propidium iodide (40 μg/mL) and RNase A (40 μg/mL). Analysis of the cell cycle was done on the LSR2 (BD Biosciences) using Diva analysis software.

ALDEFLUOR assay

The ALDEFLUOR Kit (Stem Cell Technologies) was used to isolate the population with high aldehyde dehydrogenase enzymatic activity using an LSR2 cytometer (Becton Dickinson Biosciences) as previously described (27).

Tumorsphere assay

BCLs were grown in adherent condition under abexinostat treatment (IC_{50}) or vehicle for 72 hours, then seeded as single cells in ultra-low attachment plates (Corning) at low density (1,000 viable cells per mL). Tumorspheres were grown in a serum-free mammary epithelium basal medium. The capacity of cells to form tumorspheres was quantified under microscope. Experiments were done in triplicate.

H&E and immunofluorescence staining

BCLs monolayers grown on LabTeck slides (Fisher Scientific) were fixed with 4% paraformaldehyde for 15 minutes at room temperature and stained as described in Supporting Information.

Gene expression profiling

RNA expression data were collected from our previous study (56) done with Affymetrix U133 Plus 2.0 human oligonucleotide microarrays. The data are deposited with Array Express under the accession number E-MTAB-1693. We applied supervised analysis based on volcano plot analysis, where fold-change and statistical difference

between groups were evaluated for each probe set. Probabilities were computed using linear models with empirical Bayes statistic included in the limma R package.

RNA extraction

RNA from BCLs or PDX was extracted using Mini Kit RNA extraction (Qiagen) following recommended instructions. RNA integrity was controlled by micro-analysis (Agilent).

Quantitative real-time PCR

Briefly, 5 μg of RNA extracted from BCLs or PDXs were reverse transcribed in accordance with manufacturer's instruction (Superscript II reverse transcriptase, Invitrogen). *Xist* expression level was quantified using TaqMan probes (Hs01077163_m1; Applied biosystems). β-actin (Hs99999903_m1) and glyceraldehyde-3-phosphate dehydrogenase (GAPDH; Hs03929097_g1) expression were used for normalization of data. For *Xist* quantification in PDXs, normal breast cell line HME1 was used as control. Fold-change expression was calculated using the $2^{-\Delta\Delta Ct}$ method.

Animal models

To explore the efficiency of abexinostat treatment on tumor growth, we utilized four primary human breast cancer xenografts (PDX) generated from 4 different patients (CRCM226X, CRCM311X, CRCM389X, CRCM392X). These PDXs were generated from chemo-naïve breast tumors with two $ER^-PR^-ERBB2^-$ tumors (CRCM311X at the 5th passage and CRCM392X at the 3rd passage), an $ER^-PR^-ERBB2^+$ tumor (CRCM226X at the 5th passage), an $ER^+PR^+ERBB2^-$ tumor (CRCM389X at the 4th passage). For each PDX, cells from these PDXs were transplanted orthotopically into fat pads of NOD/SCID mice without cultivation *in vitro*. We injected 1,000,000 (CRCM226X, CRCM311X, CRCM389X) or 125,000 cells (CRCM392X) per fat pads of NOD/SCID mice (with two injected fat pads per mice) and monitored tumor growth. When tumor size was approximately 150 mm^3, we initiated treatment with abexinostat alone (i.p., 12.5 mg/kg, twice a day, 5/7 days), docetaxel alone (i.p., 10 mg/kg, once a week; Sigma) or placebo injected with 20% cyclodextrin (i.p., twice a day, 5/7 days; Sigma), and 20% DMSO (i.p., once a week). Six mice (i.e., twelve tumors) were injected for each PDX and for each group. After 1, 2, and 3 weeks of treatment, two mice (i.e., four tumors) from each group were sacrificed according to ethic statements. Tumors were dissociated and cells were analyzed for the ALDEFLUOR phenotype. Cells from 3-week treated mice were reimplanted into two (CRCM226X) or four (CRCM311X) secondary NOD/SCID mice with injection of 1,000 cells for each treated tumor (i.e., four or eight injections per group).

Statistical analysis

Results are presented as the mean ± SD for at least three repeated individual experiments for each group. Statistical analyses used the R software. Correlations between sample groups and molecular parameters were calculated with the Fisher exact test or the *t* test for independent samples. The GMM was used to attribute BCLs to drug-response groups. Wilcoxon test for independent samples was used to compare different tumor sizes at different time points. The Pearson test was used to evaluate the correlation between *Xist* gene expression level measured by cDNA microarrays and qRT-PCR. The Kruskal–Wallis rank-sum test was used to compare repartition of $Xist^{low}$ and $Xist^{high}$ tumors in both BCL groups. $P < 0.05$ was considered significant.

Disclosure of Potential Conflicts of Interest

M.A. Salvador, J. Wicinski, O. Cabaud, Y. Toiron, E. Josselin, and C. Ginestier have commercial research grant from Institut de Recherches Internationale Servier. No potential conflicts of interest were disclosed by the other authors.

Authors' Contributions

Conception and design: H. Lelièvre, S. Depil, Y. Collette, D. Birnbaum, E. Charafe-Jauffret, C. Ginestier
Development of methodology: M.A. Salvador, O. Cabaud, E. Josselin, E. Charafe-Jauffret, C. Ginestier
Acquisition of data (provided animals, acquired and managed patients, provided facilities, etc.): M.A. Salvador, J. Wicinski, O. Cabaud, Y. Toiron, P. Finetti, E. Josselin, F. Bertucci, Y. Collette, D. Birnbaum, E. Charafe-Jauffret, C. Ginestier
Analysis and interpretation of data (e.g., statistical analysis, biostatistics, computational analysis): M.A. Salvador, O. Cabaud, P. Finetti, E. Josselin, F. Bertucci, Y. Collette, E. Charafe-Jauffret, C. Ginestier
Writing, review, and/or revision of the manuscript: M.A. Salvador, H. Lelièvre, L. Kraus-Berthier, S. Depil, D. Birnbaum, E. Charafe-Jauffret, C. Ginestier
Administrative, technical, or material support (i.e., reporting or organizing data, constructing databases): J. Wicinski, Y. Toiron, P. Finetti, D. Birnbaum, E. Charafe-Jauffret
Study supervision: H. Lelièvre, L. Kraus-Berthier, Y. Collette, E. Charafe-Jauffret, C. Ginestier

Acknowledgments

The authors thank the Association pour la Recherche contre le Cancer for supporting their acquisition of a cell sorter and the CRCM flow cytometry core facility and the CRCM animal core facility.

Grant Support

This study was supported by Inserm, Institut Paoli-Calmettes and grants from the Ligue National Contre le Cancer (to D. Birnbaum) and Institut National du Cancer (R. Translationnelle 2009, PL Xenotek). M.A. Salvador was supported by a fellowship from the Ministry of Research.

The costs of publication of this article were defrayed in part by the payment of page charges. This article must therefore be hereby marked *advertisement* in accordance with 18 U.S.C. Section 1734 solely to indicate this fact.

Received April 2, 2013; revised September 24, 2013; accepted September 25, 2013; published OnlineFirst October 18, 2013.

References

1. Kouzarides T. SnapShot: histone-modifying enzymes. Cell 2007; 131:822.
2. Strahl BD, Allis CD. The language of covalent histone modifications. Nature 2000;403:41–5.
3. Lane AA, Chabner BA. Histone deacetylase inhibitors in cancer therapy. J Clin Oncol 2009;27:5459–68.
4. Wicha MS, Liu S, Dontu G. Cancer stem cells: an old idea–a paradigm shift. Cancer Res 2006;66:1883–90.

5. Visvader JE, Lindeman GJ. Cancer stem cells: current status and evolving complexities. Cell Stem Cell 2012;10:717–28.
6. Liu S, Wicha MS. Targeting breast cancer stem cells. J Clin Oncol 2010;28:4006–12.
7. Cruz FD, Matushansky I. Solid tumor differentiation therapy - is it possible? Oncotarget 2012;3:559–67.
8. Mohn F, Weber M, Rebhan M, Roloff TC, Richter J, Stadler MB, et al. Lineage-specific polycomb targets and de novo DNA methylation define restriction and potential of neuronal progenitors. Mol Cell 2008;30:755–66.
9. Tollervey JR, Lunyak VV. Epigenetics: judge, jury and executioner of stem cell fate. Epigenetics 2012;7:823–40.
10. Leder A, Orkin S, Leder P. Differentiation of erythroleukemic cells in the presence of inhibitors of DNA synthesis. Science 1975;190:893–4.
11. Minucci S, Pelicci PG. Histone deacetylase inhibitors and the promise of epigenetic (and more) treatments for cancer. Nat Rev Cancer 2006;6:38–51.
12. Hrzenjak A, Moinfar F, Kremser ML, Strohmeier B, Staber PB, Zatloukal K, et al. Valproate inhibition of histone deacetylase 2 affects differentiation and decreases proliferation of endometrial stromal sarcoma cells. Mol Cancer Ther 2006;5:2203–10.
13. Yamashita Y, Shimada M, Harimoto N, Rikimaru T, Shirabe K, Tanaka S, et al. Histone deacetylase inhibitor trichostatin A induces cell-cycle arrest/apoptosis and hepatocyte differentiation in human hepatoma cells. Int J Cancer 2003;103:572–6.
14. Platta CS, Greenblatt DY, Kunnimalaiyaan M, Chen H. The HDAC inhibitor trichostatin A inhibits growth of small cell lung cancer cells. J Surg Res 2007;142:219–26.
15. Munster PN, Troso-Sandoval T, Rosen N, Rifkind R, Marks PA, Richon VM. The histone deacetylase inhibitor suberoylanilide hydroxamic acid induces differentiation of human breast cancer cells. Cancer Res 2001;61:8492–7.
16. Siegel D, Hussein M, Belani C, Robert F, Galanis E, Richon VM, et al. Vorinostat in solid and hematologic malignancies. J Hematol Oncol 2009;2:31.
17. Buggy JJ, Cao ZA, Bass KE, Verner E, Balasubramanian S, Liu L, et al. CRA-024781: a novel synthetic inhibitor of histone deacetylase enzymes with antitumor activity *in vitro* and *in vivo*. Mol Cancer Ther 2006;5:1309–17.
18. Charafe-Jauffret E, Ginestier C, Iovino F, Wicinski J, Cervera N, Finetti P, et al. Breast cancer cell lines contain functional cancer stem cells with metastatic capacity and a distinct molecular signature. Cancer Res 2009;69:1302–13.
19. Ponti D, Costa A, Zaffaroni N, Pratesi G, Petrangolini G, Coradini D, et al. Isolation and *in vitro* propagation of tumorigenic breast cancer cells with stem/progenitor cell properties. Cancer Res 2005;65:5506–11.
20. Shah RD, Jagtap JC, Mruthyunjaya S, Shelke GV, Pujari R, Das G, et al. Sodium valproate potentiates staurosporine-induced apoptosis in neuroblastoma cells via Akt/survivin independently of HDAC inhibition. J Cell Biochem 2013;114:854–63.
21. Venkataramani V, Rossner C, Iffland L, Schweyer S, Tamboli IY, Walter J, et al. Histone deacetylase inhibitor valproic acid inhibits cancer cell proliferation via down-regulation of the alzheimer amyloid precursor protein. J Biol Chem 2010;285:10678–89.
22. Harikrishnan KN, Karagiannis TC, Chow MZ, El-Osta A. Effect of valproic acid on radiation-induced DNA damage in euchromatic and heterochromatic compartments. Cell Cycle 2008;7:468–76.
23. Horwitz KB, Dye WW, Harrell JC, Kabos P, Sartorius CA. Rare steroid receptor-negative basal-like tumorigenic cells in luminal subtype human breast cancer xenografts. Proc Natl Acad Sci U S A 2008;105:5774–9.
24. Brockdorff N. Chromosome silencing mechanisms in X-chromosome inactivation: unknown unknowns. Development 2011;138:5057–65.
25. Agrelo R, Wutz A. ConteXt of change–X inactivation and disease. EMBO Mol Med 2010;2:6–15.
26. Weakley SM, Wang H, Yao Q, Chen C. Expression and function of a large non-coding RNA gene XIST in human cancer. World J Surg 2011;35:1751–6.
27. Ginestier C, Hur MH, Charafe-Jauffret E, Monville F, Dutcher J, Brown M, et al. ALDH1 is a marker of normal and malignant human mammary stem cells and a predictor of poor clinical outcome. Cell Stem Cell 2007;1:555–67.
28. Li X, Lewis MT, Huang J, Gutierrez C, Osborne CK, Wu MF, et al. Intrinsic resistance of tumorigenic breast cancer cells to chemotherapy. J Natl Cancer Inst 2008;100:672–9.
29. Menchon C, Edel MJ, Izpisua Belmonte JC. The cell cycle inhibitor p27Kip(1) controls self-renewal and pluripotency of human embryonic stem cells by regulating the cell cycle, Brachyury and Twist. Cell Cycle 2011;10:1435–47.
30. Orford KW, Scadden DT. Deconstructing stem cell self-renewal: genetic insights into cell-cycle regulation. Nat Rev Genet 2008;9:115–28.
31. Kretsovali A, Hadjimichael C, Charmpilas N. Histone deacetylase inhibitors in cell pluripotency, differentiation, and reprogramming. Stem Cells Int 2012;2012:184154.
32. Landreville S, Agapova OA, Matatall KA, Kneass ZT, Onken MD, Lee RS, et al. Histone deacetylase inhibitors induce growth arrest and differentiation in uveal melanoma. Clin Cancer Res 2012;18:408–16.
33. Schwartz BE, Hofer MD, Lemieux ME, Bauer DE, Cameron MJ, West NH, et al. Differentiation of NUT midline carcinoma by epigenomic reprogramming. Cancer Res 2011;71:2686–96.
34. Sun P, Xia S, Lal B, Eberhart CG, Quinones-Hinojosa A, Maciaczyk J, et al. DNER, an epigenetically modulated gene, regulates glioblastoma-derived neurosphere cell differentiation and tumor propagation. Stem Cells 2009;27:1473–86.
35. Debeb BG, Lacerda L, Xu W, Larson R, Solley T, Atkinson R, et al. Histone deacetylase inhibitors stimulate dedifferentiation of human breast cancer cells through WNT/beta-catenin signaling. Stem Cells 2012;30:2366–77.
36. Kong D, Ahmad A, Bao B, Li Y, Banerjee S, Sarkar FH. Histone deacetylase inhibitors induce epithelial-to-mesenchymal transition in prostate cancer cells. PLoS ONE 2012;7:e45045.
37. Lin KT, Wang YW, Chen CT, Ho CM, Su WH, Jou YS. HDAC inhibitors augmented cell migration and metastasis through induction of PKCs leading to identification of low toxicity modalities for combination cancer therapy. Clin Cancer Res 2012;18:4691–701.
38. Tsai HC, Li H, Van NL, Cai Y, Robert C, Rassool FV, et al. Transient low doses of DNA-demethylating agents exert durable antitumor effects on hematological and epithelial tumor cells. Cancer Cell 2012;21:430–46.
39. Rottenberg S, Vollebergh MA, de HB, de RJ, Schouten PC, Kersbergen A, et al. Impact of intertumoral heterogeneity on predicting chemotherapy response of BRCA1-deficient mammary tumors. Cancer Res 2012;72:2350–61.
40. Wang RH, Yu H, Deng CX. A requirement for breast-cancer-associated gene 1 (BRCA1) in the spindle checkpoint. Proc Natl Acad Sci U S A 2004;101:17108–13.
41. Adimoolam S, Sirisawad M, Chen J, Thiemann P, Ford JM, Buggy JJ. HDAC inhibitor PCI-24781 decreases RAD51 expression and inhibits homologous recombination. Proc Natl Acad Sci U S A 2007;104:19482–7.
42. Silver DP, Dimitrov SD, Feunteun J, Gelman R, Drapkin R, Lu SD, et al. Further evidence for BRCA1 communication with the inactive X chromosome. Cell 2007;128:991–1002.
43. Sirchia SM, Ramoscelli L, Grati FR, Barbera F, Coradini D, Rossella F, et al. Loss of the inactive X chromosome and replication of the active X in BRCA1-defective and wild-type breast cancer cells. Cancer Res 2005;65:2139–46.
44. Sirchia SM, Tabano S, Monti L, Recalcati MP, Gariboldi M, Grati FR, et al. Misbehaviour of XIST RNA in breast cancer cells. PLoS ONE 2009;4:e5559.
45. Vincent-Salomon A, Ganem-Elbaz C, Manie E, Raynal V, Sastre-Garau X, Stoppa-Lyonnet D, et al. X inactive-specific transcript RNA coating and genetic instability of the X chromosome in BRCA1 breast tumors. Cancer Res 2007;67:5134–40.
46. Xiao C, Sharp JA, Kawahara M, Davalos AR, Difilippantonio MJ, Hu Y, et al. The XIST noncoding RNA functions independently of BRCA1 in X inactivation. Cell 2007;128:977–89.
47. Lim E, Vaillant F, Wu D, Forrest NC, Pal B, Hart AH, et al. Aberrant luminal progenitors as the candidate target population for basal

tumor development in BRCA1 mutation carriers. Nat Med 2009;15:907–13.
48. Liu S, Ginestier C, Charafe-Jauffret E, Foco H, Kleer CG, Merajver SD, et al. BRCA1 regulates human mammary stem/progenitor cell fate. Proc Natl Acad Sci U S A 2008;105:1680–5.
49. Nagano T, Fraser P. No-nonsense functions for long noncoding RNAs. Cell 2011;145:178–81.
50. Guttman M, Donaghey J, Carey BW, Garber M, Grenier JK, Munson G, et al. lincRNAs act in the circuitry controlling pluripotency and differentiation. Nature 2011;477:295–300.
51. Prensner JR, Chinnaiyan AM. The emergence of lncRNAs in cancer biology. Cancer Discov 2011;1:391–407.
52. Yildirim E, Kirby JE, Brown DE, Mercier FE, Sadreyev RI, Scadden DT, et al. Xist RNA is a potent suppressor of hematologic cancer in mice. Cell 2013;152:727–42.
53. Neve RM, Chin K, Fridlyand J, Yeh J, Baehner FL, Fevr T, et al. A collection of breast cancer cell lines for the study of functionally distinct cancer subtypes. Cancer Cell 2006;10:515–27.
54. Kadra G, Finetti P, Toiron Y, Viens P, Birnbaum D, Borg JP, et al. Gene expression profiling of breast tumor cell lines to predict for therapeutic response to microtubule-stabilizing agents. Breast Cancer Res Treat 2012;132:1035–47.
55. Letessier A, Mozziconacci MJ, Murati A, Juriens J, Adelaide J, Birnbaum D, et al. Multicolour-banding fluorescence *in situ* hybridisation (mbanding-FISH) to identify recurrent chromosomal alterations in breast tumour cell lines. Br J Cancer 2005;92:382–8.
56. Charafe-Jauffret E, Ginestier C, Monville F, Finetti P, Adelaide J, Cervera N, et al. Gene expression profiling of breast cell lines identifies potential new basal markers. Oncogene 2006;25:2273–84.